

# Photon colliders: current and future projects

Valery Telnov

Institute of Nuclear Physics, 630090 Novosibirsk, Russia,  
and DESY, Germany

## Abstract

Photon colliders ( $\gamma\gamma$ ,  $\gamma e$ ) are based on backward Compton scattering of laser light off the high energy electrons of linear colliders. This option is considered now for all linear colliders projects. In this paper we present possible parameters of the Photon Collider at TESLA. The  $\gamma\gamma$  luminosity in the current design is determined by “geometric luminosity” of electron beams. Having beams with smaller emittances one could obtain much higher luminosity. Especially attractive is the Higgs factory (if the Higgs boson with the mass of 100-200 GeV really exists). Problems of multi-TeV photon colliders and possible solutions are also discussed.

## 1 INTRODUCTION

The unique feature of the  $e^+e^-$  Linear Colliders (LC) with the energy from hundreds GeV to several TeV which are under development now [1, 3, 2, 4] is the possibility to construct on its basis a Photon Linear Collider using the process of the Compton backscattering of laser light off the high energy electrons [5, 6, 7] (see also proceedings of the workshop on photon colliders held at Berkeley [9], 1995 and at Hamburg, 2000 [10]). The maximum energy of the

where  $E_0$  is the electron beam energy and  $\omega_0$  the energy of the laser photon. For example, for  $E_0 = 250$  GeV,  $\omega_0 = 1.17$  eV, i.e.  $\lambda = 1.06 \mu\text{m}$  (Nd:glass laser), we obtain  $x = 4.5$  and  $\omega_m = 0.82E_0$ .

The high energy photon spectrum becomes more peaked for increasing values of  $x$ . It turns out that the value  $x \approx 4.8$  is the optimum choice for photon colliders, because for  $x > 4.8$  the produced high energy photons create QED  $e^+e^-$  pairs in collision with the laser photons, and the  $\gamma\gamma$  luminosity [6, 7, 11] will be reduced. Hence, the maximum c.m.s. energy in  $\gamma\gamma$  collisions is about 80% (and 90% in  $\gamma e$  collisions) of that in  $e^+e^-$  collisions.

A typical luminosity distribution in  $\gamma\gamma$  collisions is characterized by a high energy peak and a low energy part, see section 3. The peak has a width at half maximum of about 15%. The photons in the peak can have a high degree of circular polarization. This peak region is most useful for experimentation. When comparing event rates in  $\gamma\gamma$  and  $e^+e^-$  collisions we will use the value of the  $\gamma\gamma$  luminosity in the peak region  $z > 0.8z_m$  where  $z = W_{\gamma\gamma}/2E_0$  ( $W_{\gamma\gamma}$  being the  $\gamma\gamma$  invariant mass) and  $z_m = \omega_m/E_0$ . The  $\gamma\gamma$  luminosity in this region is proportional to the geometric luminosity  $L_{geom}$  of the electron beams:  $L_{\gamma\gamma}(z > 0.8z_m) \sim 0.1L_{ee,geom}$ <sup>1</sup>. The geometric luminosity of electron beams in a  $\gamma\gamma$  collision region can be made larger than the  $e^+e^-$  luminosity because beamstrahlung and beam repulsion are absent for photon beams.

The energy spectrum of high energy photons becomes most strongly peaked if the initial electrons are longitudinally polarized and the laser photons are circularly polarized. This gives almost a factor of 3–4 increase of the luminosity in the high energy peak. The average degree of circular polarization of photons within the high-energy peak amounts to 90–95%. The sign of the polarization can easily be changed by changing the signs of both electron and laser photon initial polarizations. Linear polarization of high energy photons can be obtained by using linearly polarized laser light [8], though it is not so high as the circular polarization.

## 2 PHYSICS

Physics in  $e^+e^-$  and  $\gamma\gamma$ ,  $\gamma e$  collisions is quite similar because the same particles can be produced. However, reactions are different and can give complementary information. Some phenomena can best be studied at photon colliders due to better accuracy (larger cross-sections) or larger accessible masses (a single resonance (in  $\gamma\gamma$  and  $\gamma e$ ) or a pair of light and heavy particles (in  $\gamma e$ ). A short list of

<sup>1</sup>for a thickness of the laser target being equal to one collision length

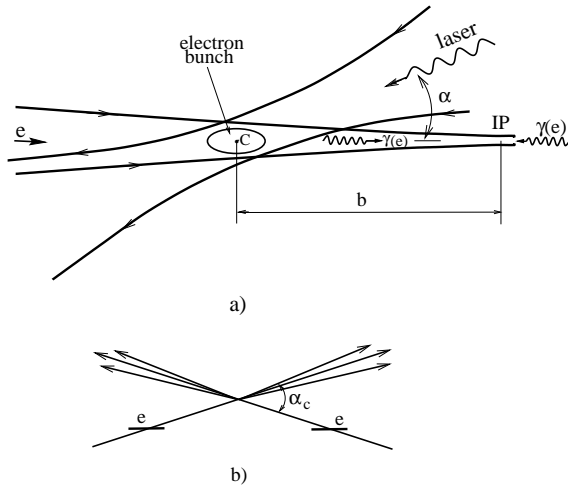


Figure 1: Scheme of  $\gamma\gamma$ ,  $\gamma e$  collider.

scattered photons is [6]

$$\omega_m = \frac{x}{x+1}E_0; \quad x \approx \frac{4E_0\omega_0}{m^2c^4} \simeq 15.3 \left[ \frac{E_0}{\text{TeV}} \right] \left[ \frac{\omega_0}{\text{eV}} \right], \quad (1)$$

processes for the physics program of the photon collider is presented in Table 1 [14]. Detail consideration of physics program at photon colliders can be found elsewhere [14].

Table 1: Gold-plated processes at photon colliders

Reaction	Remarks
$\gamma\gamma \rightarrow h_0 \rightarrow \bar{b}b$	$M_{h_0} < 160$ GeV
$\gamma\gamma \rightarrow h_0 \rightarrow WW(WW^*)$	$140 < M_{h_0} < 190$ GeV
$\gamma\gamma \rightarrow h_0 \rightarrow ZZ(ZZ^*)$	$180 < M_{h_0} < 350$ GeV
$\gamma\gamma \rightarrow H, A \rightarrow \bar{b}b$	$\mathcal{MSSM}$ heavy Higgs
$\gamma\gamma \rightarrow \tilde{f}\tilde{f}, \tilde{\chi}_i^+ \tilde{\chi}_i^-, H^+ H^-$	supersymmetric particles
$\gamma\gamma \rightarrow S[\tilde{t}\tilde{t}]$	$\tilde{t}\tilde{t}$ stoponium
$\gamma e \rightarrow \tilde{e}^- \tilde{\chi}_1^0$	$M_{\tilde{e}^-} < 0.9 \times 2E_0 - M_{\tilde{\chi}_1^0}$
$\gamma\gamma \rightarrow W^+ W^-$	anom. $W$ inter., extra dim.
$\gamma e^- \rightarrow W^- \nu_e$	anom. $W$ couplings
$\gamma\gamma \rightarrow WW + WW(ZZ)$	strong $WW$ scattering
$\gamma\gamma \rightarrow t\bar{t}$	anom. $t$ -quark interactions
$\gamma e^- \rightarrow \bar{t}b\nu_e$	anom. $Wtb$ coupling
$\gamma\gamma \rightarrow \text{hadrons}$	total $\gamma\gamma$ cross section
$\gamma e^- \rightarrow e^- X$ and $\nu_e X$	struct. functions
$\gamma g \rightarrow \bar{q}q, \bar{c}c$	gluon distr. in the photon
$\gamma\gamma \rightarrow J/\psi, J/\psi$	QCD Pomeron

### 3 THE PHOTON COLLIDER AT TESLA

The TESLA team has published the Technical Design Report just two days before our conference. The Photon Collider is included in the project, though all technical aspects, especially the laser system, should be developed in more detail in the next 2–3 years.

The resulting parameters of the photon collider at TESLA for the energy of electron beams  $2E_0 = 200, 500$  and  $800$  GeV are presented in table 2. For comparison the  $e^+e^-$  luminosity at TESLA is also included. It is assumed that the electron beams have 85% longitudinal polarization and that the laser photons have 100% circular polarization. The thickness of the laser target is one scattering length for  $2E_0 = 500$  and  $800$  GeV and 1.35 scattering length for  $2E_0 = 200$  GeV (the Compton cross section is larger), so that  $k^2 \approx 0.4$  and  $0.55$ , respectively ( $k$  is the  $e \rightarrow \gamma$  conversion coefficient). The laser wave length is  $1.06 \mu\text{m}$  for all energies. The conversion point is situated at a distance  $b = \gamma\sigma_y$  from the interaction point.

The maximum energies in  $\gamma\gamma$  and  $\gamma e$  collisions given in table 2 are somewhat lower than follow from eq.1 due to the nonlinear effects in Compton scattering. This lead to decrease of the effective value of  $x$  by a factor of  $(1 + \xi^2)$ , where the parameter  $\xi^2 = 0.15, 0.3, 0.4$  for  $2E_0 = 200, 500, 800$  GeV, respectively.

Table 2: Parameters of the photon collider at TESLA.

$2E_0$	200	500	800
$\lambda_L [\mu\text{m}]/x$	1.06/1.8	1.06/4.5	1.06/7.2
$t_L [\lambda_{scat}]$	1.35	1	1
$N/10^{10}$	2	2	2
$\sigma_z [\text{mm}]$	0.3	0.3	0.3
$f_{rep} \times n_b [\text{kHz}]$	14.1	14.1	14.1
$\gamma\epsilon_{x/y}/10^{-6} [\text{m-rad}]$	2.5/0.03	2.5/0.03	2.5/0.03
$\beta_{x/y} [\text{mm}]$ at IP	1.5/0.3	1.5/0.3	1.5/0.3
$\sigma_{x/y} [\text{nm}]$	140/6.8	88/4.3	69/3.4
<b>b [mm]</b>	2.6	2.1	2.7
$L_{ee}(\text{geom}) [10^{34} \text{cm}^{-2}\text{s}^{-1}]$	4.8	12	19
$L_{ee}(z > 0.65)$	0.03	0.07	0.095
$W_{\gamma\gamma, max} (\text{GeV})$	122	390	670
$L_{\gamma\gamma}(z > 0.8z_m, \gamma\gamma)$	0.43	1.1	1.7
$W_{\gamma e, max} (\text{GeV})$	156	440	732
$L_{\gamma e}(z > 0.8z_m, \gamma e)$	0.36	0.94	1.3
$L_{e^+e^-}, 10^{34}\text{cm}^{-2}\text{s}^{-1}$	1.3	3.4	5.8

One can see that for the same energy

$$L_{\gamma\gamma}(z > 0.8z_m) \approx \frac{1}{3}L_{e^+e^-}. \quad (2)$$

Note than cross sections in  $\gamma\gamma$  collisions are typically by one order of magnitude higher than in  $e^+e^-$  collisions.

The relation (2) is valid only for the beam parameters considered. A more universal relation is (for  $k^2 = 0.4$ )

$$L_{\gamma\gamma}(z > 0.8z_m) \approx 0.09L_{ee}(\text{geom}). \quad (3)$$

Simultaneously with  $\gamma\gamma$  collisions there are also  $\gamma e$  collisions with somewhat lower luminosity, so one can study both types of collisions simultaneously. Residual electron-electron luminosity is very small due to the beam repulsion.

The normalized  $\gamma\gamma$  luminosity spectra for  $2E_0 = 200$  and  $800$  GeV are shown in Fig. 2 [12]. The luminosity spectrum is decomposed into two parts with the total helicity of the two photons 0 and 2. We see that in the high energy part of the luminosity spectra the photons have a high degree of polarization. In addition to the high energy peak, there is a factor 5–8 higher luminosity at low energy. It is produced mainly by photons after multiple Compton scattering and beamstrahlung photons. These events have a large boost and can be easily distinguished from the central high energy events. Fig. 2 shows the same spectrum with an additional cut on the longitudinal momentum of the produced system, which suppresses the low energy luminosity to a low level.

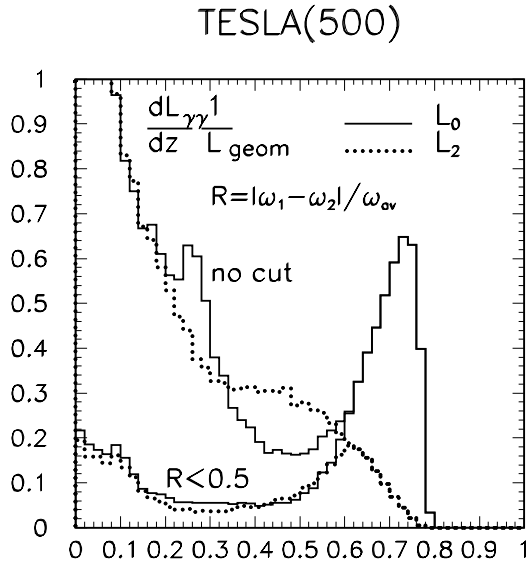


Figure 2:  $\gamma\gamma$  luminosity spectra at TESLA(500). Solid line for total helicity of the two photons 0 and dotted line for total helicity 2. Lower curves with cut on longitudinal momentum.

The normalized  $\gamma e$  luminosity spectra for  $2E_0 = 500$  GeV are shown in Fig. 3. Again, besides the high energy peak there is a several times higher  $\gamma e$  luminosity at low invariant masses. Note, that the  $\gamma e$  luminosity in the high energy peak is not a simple geometric characteristic of the Compton scattering process (as it is in  $\gamma\gamma$  collisions). For the case considered it is suppressed by a factor of 2–3, mainly due to the repulsion of the electron beams and beamstrahlung. The suppression factor depends strongly on the electron beam parameters.

For dedicated  $\gamma e$  experiments one can convert only one electron beam, increase the distance between the conversion and the interaction points and obtain a much more monochromatic  $\gamma e$  luminosity spectrum.

The  $\gamma\gamma$  luminosity distributions, including all their polarization characteristics, can be measured using processes  $\gamma\gamma \rightarrow l^+l^-$ , where  $l = e$  or  $\mu$ .  $\gamma e$  luminosity can be measured using the process  $\gamma e \rightarrow \gamma e$ .

#### 4 LUMINOSITY LIMITATIONS DUE TO BEAM COLLISIONS EFFECTS AT TESLA ENERGIES

Beam collision effects in  $e^+e^-$  and  $\gamma\gamma$ ,  $\gamma e$  collisions are different. In particular, in  $\gamma\gamma$  collisions there are no beamstrahlung or beam instabilities. Therefore, it was of interest to study limitations of the luminosity at the TESLA photon collider due to beam collision effects. The simulation [12] was done for the TESLA beams and the horizontal size of the electron beams was varied.

Fig. 4 shows the dependence of the  $\gamma\gamma$  (solid curves) and the  $\gamma e$  (dashed curves) luminosities on the horizontal beam size for several energies. The horizontal beam size was varied by changing the horizontal beam emittance keeping

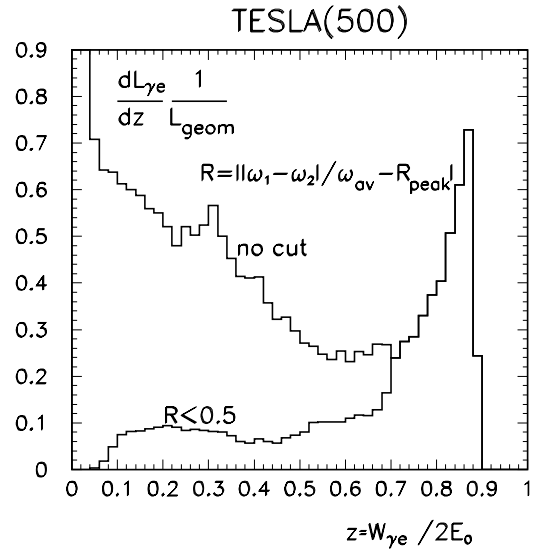


Figure 3: Normalized  $\gamma e$  luminosity spectra at TESLA(500) when the photon collider is optimized for  $\gamma\gamma$  collisions. Lower curves with cut on longitudinal momentum.

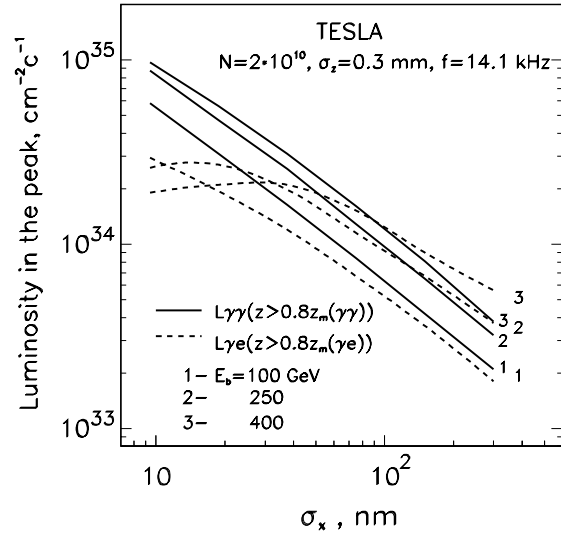


Figure 4: Dependence of  $\gamma\gamma$  and  $\gamma e$  luminosities in the high energy peak on the horizontal beam size for TESLA at various energies.

the horizontal beta function at the IP constant and equal to 1.5 mm.

One can see that all curves for the  $\gamma\gamma$  luminosity follow their natural behavior:  $L \propto 1/\sigma_x$  (values of  $\sigma_x < 10$  nm are not considered because too small horizontal sizes may introduce problems with the crab-crossing scheme). Note that while in  $e^+e^-$  collisions  $\sigma_x \approx 500$  nm, in  $\gamma\gamma$  collisions the attainable  $\sigma_x$  with the planned injector (damping ring) is about 100 nm.

In  $\gamma e$  collisions the luminosity at small  $\sigma_x$  is lower than follows from the geometric scaling due to beamstrahlung and displacement of the electron beam during the beam col-

lision.

So, we can conclude that for  $\gamma\gamma$  collisions at TESLA one can use beams with a horizontal beam size down to 10 nm (maybe even smaller) which is much smaller than that in  $e^+e^-$  collisions. Note, that the vertical beam size could also be additionally decreased by a factor of two (for even smaller electron beam size the effective photon beam size will be determined by the Compton scattering contribution). As a result, having beams with very smaller emittances, the  $\gamma\gamma$  luminosity in the high energy peak can be, in principle, several times higher than the  $e^+e^-$  luminosity.

Production of the polarized electron beams with emittances lower than those possible with damping rings is a challenging problem. There is one method, laser cooling [15, 16] which allows, in principle, the required emittances to be reached. However this method requires a laser power one order of magnitude higher than is needed for  $e \rightarrow \gamma$  conversion. This is not excluded, may be for the second generation of photon colliders.

## 5 PHOTON COLLIDER FACTORIES

We have seen in previous section that at TESLA the  $\gamma\gamma$  luminosity in the high energy peak is about 1/3 of the  $e^+e^-$  luminosity. The later is restricted by collision effects, but the  $\gamma\gamma$  luminosity at the considered energies may be further increased by one order of magnitude. Moreover, the the cross sections of most of processes at photon colliders are considerably larger. For example, already at current TESLA parameters the rate of the neutral Higgs boson  $h_0$  in  $\gamma\gamma$  collisions will be higher by a factor of 1–10 for the Higgs mass  $M_h = 120\text{--}250$  GeV [12]. The rate of charged scalars (charged Higgs bosons or supersymmetric particles expected in some theories) is higher by a factor of 8 not far from the threshold. The rate of WW pairs will be also higher approximately by the same factor. The list of examples could be continued. If methods to decrease electron beam emittances were found (the laser cooling or something else) then  $\gamma\gamma$  factories of some particles would be possible.

## 6 LASERS-OPTICS

The photon collider at TESLA requires the laser with wavelength about  $1 \mu\text{m}$ , the flash energy 5 J, duration 1.5 ps and the repetition rate 14 kHz. The average power for two beams should be about 140 kW. All parameters are reasonable for exception of the repetition rate (average power). To overcome this problem each laser bunch in the scheme considered for TESLA, see Fig.5, is used for the  $e \rightarrow \gamma$  conversion many times (12 in the current design) [12]. The laser pulse is sent to the interaction region where it is trapped in an optical storage ring. This can be done using Pockels cells (P), thin film polarizers (TFP) and 1/4-wavelength plates ( $\lambda/4$ ). The same laser can be used for the whole range of the TESLA energies.

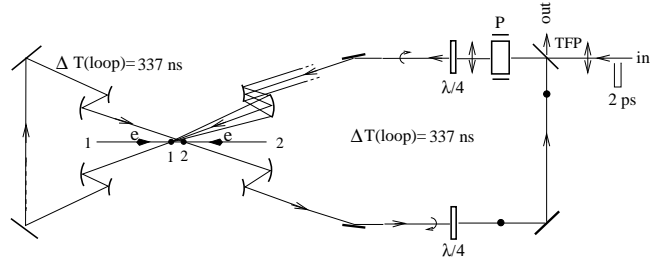


Figure 5: Optical trap (storage ring)

## 7 MULTI-TeV PHOTON COLLIDERS

The energy region of TESLA, JLC, NLC colliders (c.m.s. energy below about one TeV) is perfectly suited for photon colliders because the required laser wave length lies in the region of most powerful solid state lasers, the flash energy is quite reasonable and collision effects do not restrict the  $\gamma\gamma$  luminosity.

At multi-TeV linear colliders, such as CLIC, with the c.m.s. energy of 5 TeV there are many additional problems:

1. the required laser wavelength is about  $10 \mu\text{m}$ ;
2. to avoid nonlinear effects in Compton scattering (they become more important with increase of the wavelength) one has to use a laser with several time larger flash energy;
3. the electron bunch train is too short for multiple use of the laser bunches;
4. collisions effects (conversion of the high energy photon into the  $e^+e^-$  pair in the field of the opposite electron beam) leads to restriction of the  $\gamma\gamma$  luminosity.

All these problems have been analyzed recently in ref.[13]. The following solutions were suggested:

1. to avoid the problem of nonlinear effects in Compton scattering the “traveling laser focus” can be used, see Fig.6. In this case electrons are collided with laser photons at a long distance and the density of laser photons in the laser focus can be lower. The required flash energy may be lower by one order of magnitude. This can be done using the chirped laser pulses.
2. to reduce the beam field at the interaction point (where high energy photons are collided) it is suggested to split the electron beams as it is shown in Fig.7.

Electron beams are tilted around the collision axis by some relative angle  $\phi \sim \mathcal{O}(0.1)\sigma_y/\sigma_x$ . Having initial displacement each of the electron beams will be split during the collision in two parts. If the transverse deflection during the beam collision,  $\Delta > \sigma_x$ , then the maximum field in the region of high energy photons (at  $x \sim \sigma_x$ ) is

$$B_r = B_b(\sigma_x/\Delta)^2 \propto \sigma_x.$$

So, with the decrease of  $\sigma_x$ , the  $\gamma\gamma$  luminosity grows but the field at the interaction region decreases! This effect works better when beams are longer. The idea is interesting and worth more detailed consideration. It may not work due to necessity of very good stabilization of the vertical beam position, that is very difficult for the CLIC with short bunch train.

Other method is to use the plasma lens between the conversion and interaction points. Electron beams after conversion will be defocused to a large spot size and the beam field near the axis (where high energy photons travel will be suppressed). Such idea was considered for  $\gamma e$  colliders in ref.[17].

Note, that if the multi-TeV photon collider uses the beams with same transverse sizes as for  $e^+e^-$  collider then the problem with coherent pair creation is not important, that is because for any beam field the probability of beamstrahlung is several times higher than the probability of coherent pair creation. For  $\gamma\gamma$  collisions one can use electron beams with the horizontal beam size at least 3 times lower than for  $e^+e^-$  collisions. The corresponding  $\gamma\gamma$  luminosity in the high energy peak will be about 20-30% of  $e^+e^-$  luminosity, this is acceptable because the cross sections in the  $\gamma\gamma$  collisions are typically by one order of magnitude higher than in  $e^+e^-$  collisions.

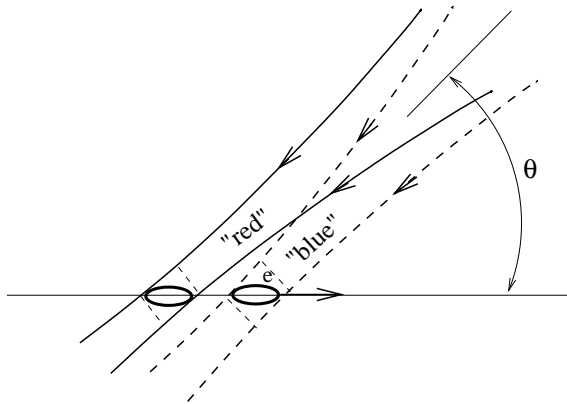


Figure 6: Traveling laser focus at the conversion region. The laser focus follows position of the electron beams.

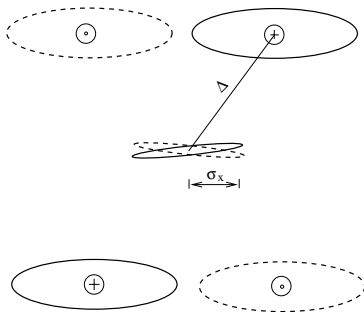


Figure 7: Idea of suppression of coherent pair creation at photon colliders.

In conclusion, photon colliders is a very promising direction of the particles physics. This option is included in the projects of the next linear colliders. At the energies of several hundreds GeV the  $\gamma\gamma$  luminosity may be very high, especially if some methods of electron beams production with very small emittance were found, and factories of various particles can be considered in future. For multi-TeV energies there are several problems, especially with lasers, which can be overcome, in principle, but need special developments.

## 8 REFERENCES

- [1] *Zeroth-Order Design Report for the Next Linear Collider* LBNL-PUB-5424, SLAC Report 474, May 1996.
- [2] *Technical Design Report*, DESY 2001-011, ECFA-97-182.
- [3] *JLC Design Study*, KEK-REP-97-1, April 1997.
- [4] R.W. Assmann et al., CERN-2000-008, 2000.
- [5] I. Ginzburg, G. Kotkin, V. Serbo, V. Telnov, *Pizma ZhETF*, **34** (1981) 514; *JETP Lett.* **34** (1982) 491. (Prep. INP 81-50, Novosibirsk, 1981).
- [6] I. Ginzburg, G. Kotkin, V. Serbo, V. Telnov, *Nucl. Instr. & Meth.* **205** (1983) 47.
- [7] V. Telnov, *Nucl. Instr. & Meth.* **A 294** (1990) 72.
- [8] I. Ginzburg, G. Kotkin, S. Panfil, V. Serbo, V. Telnov, *Nucl. Instr. & Meth.* **219** (1984) 5.
- [9] *Proc. of Workshop on Gamma-Gamma Colliders*, Berkeley CA, USA, 1994, *Nucl. Instr. & Meth.* **A 355** (1995).
- [10] *Intern. Workshop on High Energy Photon Colliders*, To be published in *Nucl. Instrum. Meth. A*, <http://www.desy.de/~gg2000>.
- [11] V. Telnov, *Nucl. Instr. & Meth.* **A 355** (1995) 3.
- [12] V.I. Telnov, *Proc. Intern. Workshop on High-Energy Photon Colliders*, Hamburg, Germany, 14-17 Jun 2000. Submitted to *Nucl. Instr. Meth. A*, hep-ex/0010033.
- [13] V.I. Telnov, *Proc. Intern. Workshop on High-Energy Photon Colliders*, Hamburg, Germany, 14-17 Jun 2000. Submitted to *Nucl. Instr. Meth. A*, hep-ex/0012047.
- [14] E. Boos et al., *Proc. Intern. Workshop on High-Energy Photon Colliders*, Hamburg, Germany, 14-17 Jun 2000. Submitted to *Nucl. Instr. Meth. A*, hep-ph/0103090.
- [15] V. Telnov, SLAC-PUB-7337, *Phys. Rev. Lett.*, **78** (1997) 4757, erratum *ibid* 80 (1998) 2747, e-print: hep-ex/9610008.
- [16] V. Telnov, *Nucl. Instr. and Meth.* **A 450** (2000) 63, hep-ex/0001029.
- [17] S. Rajagopalan, D.B. Cline, P. Chen. 1995. *Nucl. Inst. Meth.* **A357** (1995) 1.